X-490-71-54
PREPRINT

EXPERIMENTAL RESULTS OF SIMULTANEOUS MEASUREMENT OF IONOSPHERIC AMPLITUDE VARIATIONS OF 136 MHz AND 1550 MHz SIGNALS AT THE GEOMAGNETIC EQUATOR

E. E. CRAMPTON, JR.
W. B. SESSIONS

JANUARY 1971

GSFC — GODDARD SPACE FLIGHT CENTER —
GREENBELT, MARYLAND

EXPERIMENTAL RESULTS OF SIMULTANEOUS MEASUREMENT OF IONOSPHERIC AMPLITUDE VARIATIONS OF 136 MHz AND 1550 MHz SIGNALS AT THE GEOMAGNETIC EQUATOR

Prepared By

E. E. Crampton Jr. and W. B. Sessions

Westinghouse Electric Corp.
for
NASA Goddard Space Flight Center

7 January 1971

EXPERIMENTAL RESULTS OF SIMULTANEOUS MEASUREMENT OF IONOSPHERIC AMPLITUDE VARIATIONS OF 136 MHz AND 1550 MHz SIGNALS AT THE GEOMAGNETIC EQUATOR

Prepared By

E. E. Crampton Jr. and W. B. Sessions

Westinghouse Electric Corp.
for
NASA Goddard Space Flight Center

7 January 1971

TABLE OF CONTENTS

		Page
1.0	INTRODUCTION	1
2.0	EXPERIMENT DESCRIPTION	1
	2.1 ATS-5 Orbital Considerations	2
	2.2 Data Acquisition Equipment	2
3.0	DATA REDUCTION TECHNIQUES	3
4.0	EXPERIMENTAL RESULTS	5
	4.1 General	5
	4.2 Geophysical Dependence	6
	4.3 Frequency Dependence	7
	4.4 Absolute Fading Depths	9
	4.5 Observed Fade Durations	9
5.0	SUMMARY AND CONCLUSIONS	12
6.0	APPENDIX	23

ACKNOWLEDGEMENTS

This paper represents the cooperation of a number of people who helped formulate, conduct, and analyze the results of this experiment. To this end the authors wish to thank the personnel of the Institute Geofisco Del Peru at the Ancon, Peru station, without whose aid this experiment could not have been performed. We are particularly grateful to Mr. D. Rau of the Westinghouse Electric Corporation for his assistance in the initial setup and alignment of the ground receiving equipment and to Messrs. E. J. Mueller and C. W. Wernlien of Westinghouse for their many helpful comments in preparing this paper. We are also most grateful to Mr. Tom Golden of the Goddard Space Flight Center for his guidance and many useful critiques. A note of thanks is also expressed to Mr. J. Baker, Assistant Project Manager, NETCOS Program, for providing the opportunity to perform this experiment.

1.0 INTRODUCTION

This report has been prepared to present the signal amplitude fading characteristics noted during the simultaneous measurement of the 136.44 MHz INTELSAT I (Early Bird) signal and 1550 MHz ATS-5 signal at Lima, Peru. Twenty three hours of data collected during the period from 29 Sept. 1970 to 29 Oct. 1970 has been analyzed and comparisons between the two frequency bands made. The data retrieval technique utilized was the manual reduction of information from strip chart recordings.

This data was collected as part of a continuing experiment to provide information on VHF and L-Band scintillation fading characteristics in the equatorial regions. The lack of information at VHF and L-Band frequencies in the equatorial region makes a program of this nature desirable to provide the satellite communication system designer with the technical data to determine optimum spectrum bands and to determine fade margins required for desired system reliabilities. Data is also being collected at Quito, Ecuador from the ATS-5 136.47 MHz and 1550 MHz outputs. Automated data programs are also being developed to extract the statistical characteristics from the received data.

2.0 EXPERIMENT DESCRIPTION

VHF and L-Band signals from INTELSAT I and ATS-5 synchronous satellites were received by the Geophysical Institute of Peru satellite tracking station at Ancon, Peru. Ancon, Peru was selected as the data collection location for several reasons. Among these are that its location on the geomagnetic equator, the availability of suitable equipment, and the presence of interested ionospheric researchers at the Geophysical Institute

of Peru. The geodedic location of Ancon is at latitude 77° 9' 01.77" W and longitude 11° 46' 44.43" S. Elevation angles during the tests for ATS-5 was 55° while INTELSAT I ranged from 49° to 52°.

2.1 ATS-5 Orbital Considerations

The ATS-5 spacecraft was intended to be gravity gradient stabilized in a synchronous orbit. As such, it was equipped with a high gain L-band transmit/receive antenna whose half power beamwidth was sufficient to illuminate the earth. A synchronous orbit was achieved, although technical difficulties during the spacecraft separation phase of the launch resulted in a spin stabilized spacecraft with a spin period of about 790 ms about an axis of spin approximately parallel with the earth's axis. The spacecraft antenna pattern thus sweeps across the earth each spin period, illuminating each point within its area of coverage for about 52 ms (to the half-power points).

The time variation due to the ATS-5 spin results in the L-Band data being collected in energy bursts as the spacecraft antenna pattern sweeps across the ground receiving system (see figure 1). The signal amplitude variations can be observed on the strip chart recordings by measuring the peaks of the signal appearing at the spin rate.

2.2 Data Acquisition Equipment

The L-band equipment consists of a 4' parabolic dish with a circular feed, a preamplifier/downconverter and an RF calibration system. This equipment receives ATS-5 L-band signals and converts them to approximately 136.5 MHz. This signal is fed to a Bendix Mod 1 telemetry receiver. The AGC from the third IF of this receiver is recorded on magnetic tape and on strip

charts. The VHF signal level was simultaneously recorded on the same magnetic tape and strip charts using coherent AGC from Interstate tracking filters. The VHF receiving system used a Taco 9 element yagi array, Bendix Mod 1 receivers and Interstate tracking filters. The Ancon "East" telemetry antenna was used for receiving the INTELSAT I VHF telemetry carrier at 136.44 MHz at a level of about -123 dbm .

The equipment configurations for the tests are shown in the appendix in figures A-6 and A-7. Receiver bandwidth for L-band was set to 10 KHz and an AGC time constant of approximately 33 milliseconds was used. The VHF carrier was tracked in a 25 Hz bandwidth. The INTELSAT I VHF signal provided a C/N ratio of 35 db which yielded good data for fades up to 27 db depth. The signal level from ATS-5 provided a C/N ratio of 16 db in the L-band receiving system giving good data for fade depths of 10 db.

The AGC was recorded on a FR600 magnetic tape recorder at 3 3/4 inches per second. The AGC was also recorded on a Sanborn hot pen chart recorder. Speed was 1 mm/sec or 10 mm/sec depending on fading conditions. Short runs at 100 mm/sec were made to allow verification of the shape of the L-band antenna pattern. The Sanborn recorder calibrations were made at 1 to 2 hour intervals. All test periods had pre and post pass calibrations.

Short plus long term drift was less than 0.5 db/2 hours in the poorest system (VHF). The sum of wow, flutter and hum on the magnetic tape causes less than 0.3 db uncertainty on the poorest calibration step. AGC linearity is such that the largest voltage step representing 5 db is not more than 2 times the smallest voltage step representing 5 db.

3.0 DATA REDUCTION TECHNIQUES

The manual reduction used for compiling the graphs presented in this paper utilized strip chart recordings as shown in figure 1. Chart speed of 1 mm/sec was used whenever there was no scintillation evident. Chart speed was raised to 10 mm/sec whenever scintillation occurred on either VHF or L-Band signals. In the manual data processing, the data was considered as "scintillating" whenever the peak-to-peak VHF signal fluctuations exceeded 2 db or L-band signal fluctuation exceeded 0.5 db.

Each strip chart received from the Ancon station was given a summary review to determine invalid data periods. An example of a strip chart summary is shown in the Appendix. In reading the record care was taken to note factors in these summaries which would lead to erroneous results. During reduction of the strip charts, time periods which could be attributed to antenna pointing adjustments, frequency retuning and calibration intervals were deleted. Mechanical problems or other times where data seemed unreliable due to other causes were also eliminated from the analysis.

The reduction process first "sliced" the data into various received power levels. These levels in the L-band reduction were taken in one db increments. In the VHF reduction, the increments were 5 db with smaller increments (2 or 3 db) taken around the median of each strip chart.

After the "slicing" process, the duration of time the received signal was below a certain power level was recorded each time the signal faded below that particular level. The resolution in the VHF reduction was 1/2 second while L-band resolution was 1 spin period or 0.783 seconds. By

summing the total time of each fade for each power level a cumulative amplitude distribution could be obtained. Also by filing the length of time of each fade into time duration categories or bins, the dwell time probability curves could be obtained for each power level.

The cumulative amplitude distribution was then plotted for each strip chart on Rayleigh probability paper. The 50% probability level was thus obtained. The data was combined by normalizing to the modal value of the power level corresponding to these 50% probability points. The dwell time probability curves and cumulative amplitude probability curves were then plotted for all data analyzed.

4.0 EXPERIMENTAL RESULTS

4.1 General

The VHF and L-band Equatorial Scintillation Experiment was originally designed to examine the frequency dependence of scintillation fading. For this reason the time blocks were selected in the hope of taking data during intervals when scintillation fading was highly probable, at least at VHF. Based on data reported by Golden[1] and Aarons, etal[2], the periods about the equinoxes show the highest scintillation activity at VHF. Furthermore, most of this activity occurs between 20:00 local mean time and 05:00 local mean time at a South American station. Accordingly, the data presented in this report represents the results of sampling signals from a geostationary satellite in time blocks starting somewhere between 19:00 and 01:00 local time (00:00 to 06:00 GMT) just after the autumnal equinox in 1970. (29 September through 29 October.) A summary of the test runs is shown in Table 1.

While it is desireable to formulate a model to predict long term scintillation statistics to help in designing satellite communication systems, a proper model cannot be deduced from these data due to the restricted sample size. The relative severity of microwave scintillation effects points up the urgent need for further experimentation in this area.

4.2 Geophysical Dependence

The results of any ionospheric scintillation study have been shown by Aarons and Allen[3], and other authors, to vary with certain parameters which are used to characterize the ionosphere's magnetic anomalies and level of ionization during the measurement interval. Allen and Aarons have investigated the correlation between scintillation index and geomagnetic activity and correlation between scintillation index and sunspot number. They show, for a sub-auroral ionospheric intersection, that the mean value of the 113 MHz scintillation index increases with the geomagnetic activity, as measured by K_{FR}, ΣK_p, and A_p. These parameters are defined in Table 1.

Aarons, Allen et al[2] have concluded that the scintillation index may not be correlated with the geomagnetic activity in equatorial regions. The data in Table 1 generally agrees with this conclusion since there appears to be no clear correlation between the scintillation fading depth exceeded 5% and 1% of the time and the ΣK_p and A_p values.

The table also shows a lack of correlation between the scintillation fade depth and the daily sunspot numbers (adjusted to the Wolf scale). This is not unexpected since Aarons et al[2] indicate a general correlation to the twelve month running smoothed sunspot index which is not represented by the daily indices R_Z and R_A' in Table I.

The sub-ionospheric intersection points for ATS-5 and INTELSAT I are slightly different, and the elevation angles are slightly different, but these factors should not influence the long-term scintillation fading statistics. The important parameters i.e., (1) geomagnetic latitudes of the intersection are essentially zero degrees for both paths, and (2) the two elevation angles are both well above 45° and within 5° of each other. Statistically, these small differences at high elevation angles should not affect the comparison of results.

4.3 Frequency Dependence of Statistics of Scintillation Fading

Figure3 shows cumulative amplitude distributions, at both VHF and L-band, of received signal for all data points. For ease of comparison, both curves have been scaled to a 0 db median level. As can be seen, at 95% time availability the VHF data shows 5.5 db fading below median while the L-band signal only shows 0.8 db fading.

At 99% time availability, the fading below median at VHF is 10 db, while that at L-band is only 1.5 db. For both the 95% and 99% time availabilities the ratio of these results is approximately 6.7. Since the ratio of frequencies is 1550/136 = 11.4, while the ratio of fading depths (in db) is only 6.7, the indicated frequency dependence of scintillation fading is f to the minus 0.78 power for the total data sample.

Table 2 is a pass by pass summary of the ratio of the db fading below median for 5% and 1% of the time at VHF and L-band. A 1/f dependence would give a ratio of 11.5, a $1/f^{0.5}$ relation would given a ratio of 3.4, and a $1/f^{0.78}$ would give a ratio of 6.7. In all but 5 of the 21 results given for 95% availability, the frequency dependence was less than 1/f. The largest ratio (15) would indicate a frequency dependence of $1/f^{1.1}$, while the smallest (1.4) would indicate a dependence of $1/f^{0.14}$.

Figure 5 shows a scatter diagram of the exponent of frequency dependence as a function of the depth of VHF scintillation fading for each test run. It may be seen that a striking relationship exists between the depth of fade and the exponent. These results show that the exponent of the frequency dependence decreases as the fading decreases which is contradictory to the relationship experienced at high and mid-latitutde stations by others[2][3]. Since the frequency dependence in the equatorial region is still rather uncertain[5] it is not known whether the dependence depicted in Figure 5 is characteristics of equatorial scintillation or due to one or more of the following.

a) Lack of resolution of the L-band measurements in the experiment,

b) Fade depths were derived from the cumulative distribution rather than from Scintillation Index used by those reporting the high and mid-latitude data.

c) Inadequate statistical sample in the individual experimental test runs.

It would appear that (a) should be weighted as the most probable cause for the low values of VHF fading, i.e., 4 db or less. Golden (4) reports similar

results in data taken at Quito, Equador during the period May to September, 1970, wherin the scintillation effects varied with a relationship between $1/f$ and $1/f^{.5}$ where f is the ratio of f_{hi}/f_{low}. The relationship of the exponent of frequency dependence to depth of VHF fades as depicted in figure 5 was not mentioned in the reference.

4.4 Absolute Fading Depths

Although not apparent in figure 3 and tables 1 and 2, some scintillation of significant magnitude was observed on L-band. Figure 2 shows the time of large L-band scintillation. These scintillations generally occurred during periods of severe VHF scintillation, were as much as 5 db, peak-to-peak, and lasted for relatively short periods. The maximum VHF scintillation exceeded the dynamic range of the receiver which indicated at least 27 db peak-to-peak. Figure 2 shows db ranges of peak-to-peak signal fluctuations over the total time span of analyzed data. The letter notation indicates the severity of scintillation. As can be seen, the range of VHF variations exceeding 5 db occurred approximately 50 percent of time. The range of L-band variations exceeded 1.5 db only 15 percent of time. Also VHF scintillation was present at all times when L-band variations were noted. However, there were periods when VHF scintillations were observed with the absence of L-band variations. It can be seen that in all instances the VHF fluctuation range was greater than the L-band range during the same interval.

4.5 Observed Fade Duration Statistics

The probability that, for a given fade depth, a single fade would have a duration less than a specified value is shown in figure 4. Data is presented both for the VHF signal and the L-band signal.

Earlier work,[2] at 136 MHz, showed that for a mid-latitude site (Hamilton, Massachusetts) there was a 40% probability that 3 db fades would last less than 10 seconds. Likewise, there was a 65% probability that 6 db fades would last less than 10 seconds. The results of that study cannot be directly compared with the results presented in figure 4 because:

1) The data in figure 4 is for 2 db, 4 db, and 8 db fade depths. It would be necessary to interpolate between these curves to obtain a 3 db or a 6 db curve.

2) The time resolution in the earlier work was relatively course. It is difficult to see any significant difference between the results for 3 db fades and those for 6 db fades.

There are some interesting results evident in figure 4 on the relative duration of fades at VHF and L-band. For 10% of the time where fades exceeded 2 db, they lasted at least 13 seconds at VHF. At L-band, when the 2 db fades occurred, they lasted at least 11.5 seconds for 10% of the fades. This would indicate that the fade durations of shallow (2 db) fades were essentially the same at both frequencies. It should be understood that this does not mean that the probability of seeing a 2 db fade is the same at VHF and L-band. This conditional distribution only indicates that, given a 2 db fade, the duration of the fade is approximately the same at both frequencies 90% of the time.

As the depth of fading increases, the duration of individual fades decreases. At VHF, there was a 90% probability of 2 db fades lasting as much as 11.5 seconds while there was a 90% probability that 8 db fades would last 6 seconds or less. This is in general agreement with the earlier work[2]

mentioned above. At L-band, there was a 90% probability that 1 db fades would last as much as 16 seconds, and there was a 90% probability that 3 db fades would last 3 seconds or less.

The frequency dependence of fade durations becomes more apparent as the depth of VHF fading increases. The 8 db fades at VHF had durations greater than those of the 3 db L-band fades. This would indicate that the duration of deep fades decreases rapidly with increasing frequency. Using the 90% level for fade durations, VHF fade durations were as much as 12 seconds, as compared with a maximum of 3 seconds for the L-band fades. Conversely, there was only a 10% probability that 3 db fades would last more than 3 seconds at L-band while there was a 60% probability that a 3 db VHF fade would last more than 3 seconds.

In summary, fade durations at low fade depths (2 db or less) are approximately the same for 90% of these fades. However, as the depth of fading increases, the VHF fades are considerably longer than L-band fades of the same depth.

5.0 SUMMARY AND CONCLUSIONS

This experiment provides for the first time detailed data on a reasonable number of hours of simultaneous VHF and L-band equatorial scintillation data. The data was taken close to the autumnal equinox and during the evening hours when significant fading was expected. This was done purposely since the primary objective of the experiment was to investigate the frequency dependency during scintillated periods rather than obtain long term scintillation fading statistics.

The data was compared to daily sunspot numbers and geomagnetic activity indicies wherein no significant correlation was apparent. The frequency dependence was investigated and a relationship between the exponent of the frequency dependence and fading depth was observed. The higher fading depths (in the order of several db for 1% to 5% of the time) tended toward a 1/f dependence. Shallow fading (in the order of 2 db or less for 1% to 5% of the time) exhibited frequency dependence exponent scattered between about 0.6 down to 0.14. The overall experimental sample 23 hours indicated a frequency dependence exponent of minus 0.78. These results are in disagreement with previously report frequency dependencies at mid and high-latitudes and should be considered inconclusive until the resolution of the L-band data and adequacy of the statistical sample is investigated. Also, the effect on the frequency dependence exponent by using the cumulative distribution rather than scintillation index needs to be investigated.

Absolute fading depths of at least 27 db peak-to-peak were observed at VHF. Depths of 5 db peak-to-peak were observed at L-band. VHF scintillation fading was present at all times when L-band variations were noted; however there were periods when VHF scintillations were observed with the absence of L-band variations.

Fade durations were investigated and it was found that the equatorial VHF fade duration statistics generally were about the same as those observed at higher latitude stations. One significant finding in the equatorial data was that at low fade depths (2 db or less), the durations are about the same at L-band, but as the depth of fade increases, the VHF fades tended to be considerably longer than L-band fades for the same depth.

REFERENCES

1. Golden, T. Ionospheric Distortion of Minitrack Signals in South America, Report No. X-525-68-54, February 1968, Goddard Space Flight Center, Greenbelt, Maryland.

2. Aarons, J, Allen, T. J., Mullen, J. P., Whitney, H. E., Elkins, T. J., Klobuchar, J. A., A Survey of Scintillation Data and its Relationship to Satellite Communications, Radio Astronomy Branch, Air Force Cambridge Research Laboratory, August 1969.

3. Allen, R. S., "Morphology of Fading of Radio Waves Traversing the Auroral Ionosphere," Ionospheric Radio Communications, pp. 294-315, Plenum Press, 1968

4. Golden, T. S. A Note on Equatorial Ionospheric Scintillation at 136 MHz and 1550 MHz, Goddard Space Flight Center Document X-520-70-397, October 1970.

5. Wernlein, C. E., Summary Report-1540 to 1660 MHz Propagation Between Geostationary Satellites and Aircraft, Revised 20 November 1970, ASTRA/BID

6. Mueller, E. J., Summary Report - Scintillation, Polarization, and Multipath Effects on VHF Propagation Between Geostationary Satellites and Aircraft, Revised December 1970, ASTRA/BID.

7. Whitney, H. E., Interim Report on Scintillation Analysis of ATS-3 Data From Sagamore Hill, Huancayo, and Narssarssuag, Air Force Cambridge Research Laboratories, Bedford, Mass.

TABLE 1: SUMMARY OF TEST RUNS WITH SUNSPOT AND MAGNETIC INDICES

Day	Time (GMT)	Run Duration (Minutes)	Fade (dB) L-Band 95%	L-Band 99%	VHF 95%	VHF 99%	R_Z	R_A'	ΣK_p	A_p
9/29	0110	49	0.6	1.0	7.5	12.5	81	89	9	5
9/29	0231	11	0.7	0.9	1.5	2.2				
9/29	0250	65	0.4	0.6	1.5	2.5				
9/29	0427	75	No scintillation							
10/2	0345	41	0.6	-	7.7	14.0	56	62	18	9
10/2	0442	51	No scintillation							
10/6	0137	91	1.2	-	8.0	12.0				
10/6	0353	88	1.5	-	8.0	11.5				
10/7	0045	50	1.0	-	9.2	-	52	63	12	6
10/7	0201	72.5	0.5	1.5	7.5	13.0	71	75	7-	4
10/8	0021	41	0.7	1.2	2.6	4.3	72	80	4-	2
10/8	0135	24	0.6	1.0	6.2	9.4				
10/8	0208	14	1.5	-	10.5	-				
10/8	0413	25	1.1	1.9	7.2	11.7				
10/9	0017	98	No scintillation				67	89	3+	2
10/9	0214	91	No scintillation							
10/9	0412	73	No scintillation							
10/10	0020	65	0.3	0.6	2.1	3.5	72	95	13.0	7
10/10	0157	28	1.0	-	9.0	15.0				
10/10	0212	43	0.7	1.2	10.4	15.0				
10/10	0302	43	0.8	-	7.5	-				
10/10	0348	52	-	-	9.0	15.0				

TABLE 1: SUMMARY OF TEST RUNS WITH SUNSPOT AND MAGNETIC INDICES (Continued)

Day	Time (GMT)	Run Duration (Minutes)	Fade (dB) L-Band 95%	L-Band 99%	VHF 95%	VHF 99%	R_Z	R_A'	ΣK_P	A_P
10/10	0540	18	-	-	10.5	20.0	72	95	13.0	7
10/28	0435	49	0.7	1.0	10.5	-	130	146	22+	15
10/29	0220	37	0.5	1.0	4.4	6.7	138	151	21-	13
10/29	0516	46	1.0	-	4.8	-				

NOTES:

(1) $R_Z = K (10g + s)$

where R_Z is daily index determined at Zurich, Switzerland

g = number of sunspot groups

s = total number of distinct spots

K depends on observer and is intended to affect the conversion to the scale originated by Wolf.

(2) R_A' is similar to R_Z except it is determined from observations in the America's.

(3) K_p is the sum of eight 3 hour K_p indices for the day.

(4) A_p is the daily world index derived from eight values of K_p

(5) Data on R_Z, R_A', ΣK_P and A_P are taken from Solar-Geophysical Data (Prompt Reports) U.S. Dept of Commerce National Oceanic and Atmospheric, Boulder, Colo.

TABLE 2 FREQUENCY CORRELATION OF INDIVIDUAL PASSES

Day of Run	95% TIME AVAILABILITY				99% TIME AVAILABILITY			
	L-Band	VHF	db Ratio	n*	L-Band	VHF	db Ratio	n*
9/29	.6	7.5	12.5	1.04	1.0	12.5	12.5	1.04
9/29	.7	1.5	2.15	.377	0.9	2.2	2.45	.37
9/29	.4	1.5	3.75	.546	0.6	2.5	4.15	.585
10/2	.6	7.7	12.9	1.05				
10/6	1.2	8.0	6.65	.78				
10/6	1.2	8.0	5.35	.69				
10/7	1.0	9.2	9.2	.912				
10/7	0.5	7.5	15	1.11	1.5	13.0	8.65	.878
10/8	0.7	2.6	3.7	.54	1.2	4.3	3.6	.528
10/8	0.6	6.2	10.3	.96	1.0	9.4	9.4	.92
10/8	1.5	10.5	7.0	.80				
10/8	1.1	7.2	6.5	.77	1.9	11.7	6.15	.746
10/10	0.3	2.1	7	.80	0.6	3.5	5.85	
10/10	1.0	9.0	9	.904				
10/10	0.7	10.4	15	1.11	1.2	15.0	12.5	1.04
10/10	0.8	7.5	9.4	.92				
10/28	0.7	10.5	15	1.11				
10/29	0.5	4.4	8.8	.89	1.0	6.7	6.7	.78
10/29	1.0	4.8	4.8	.645				

*n is the exponent of frequency dependency

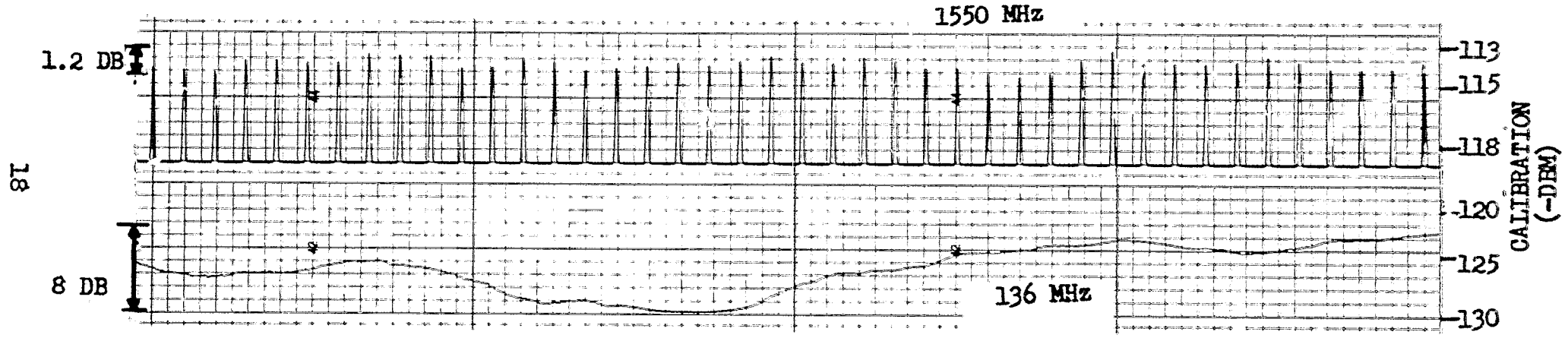

Figure 1 Ionespheric Disturbance of VHF and L-Band Signals on 10 Oct. 1970

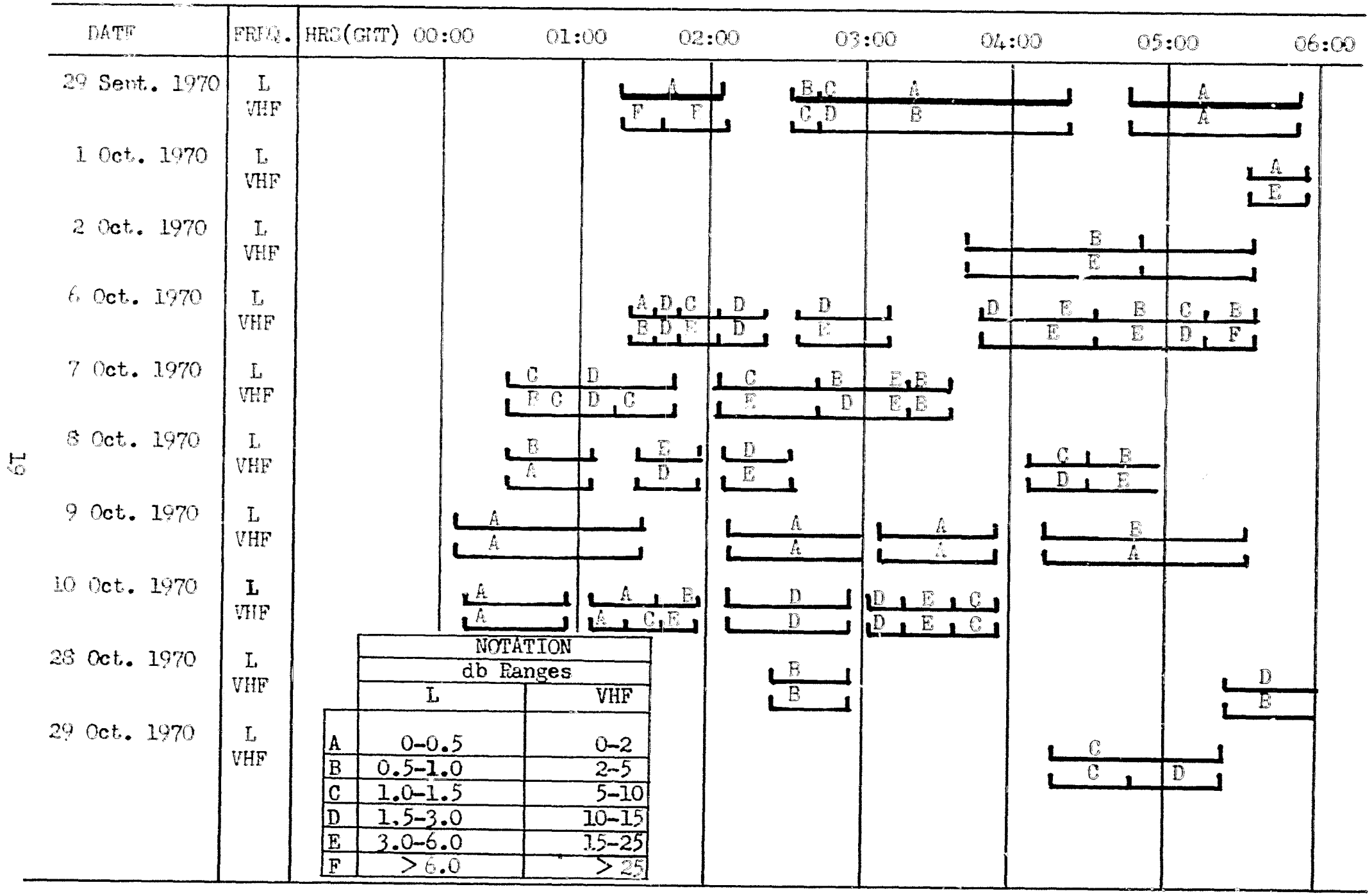

Figure 2 Peak-to-Peak Range of the VHF and L-Band Received Signal Levels for all Time Analyzed

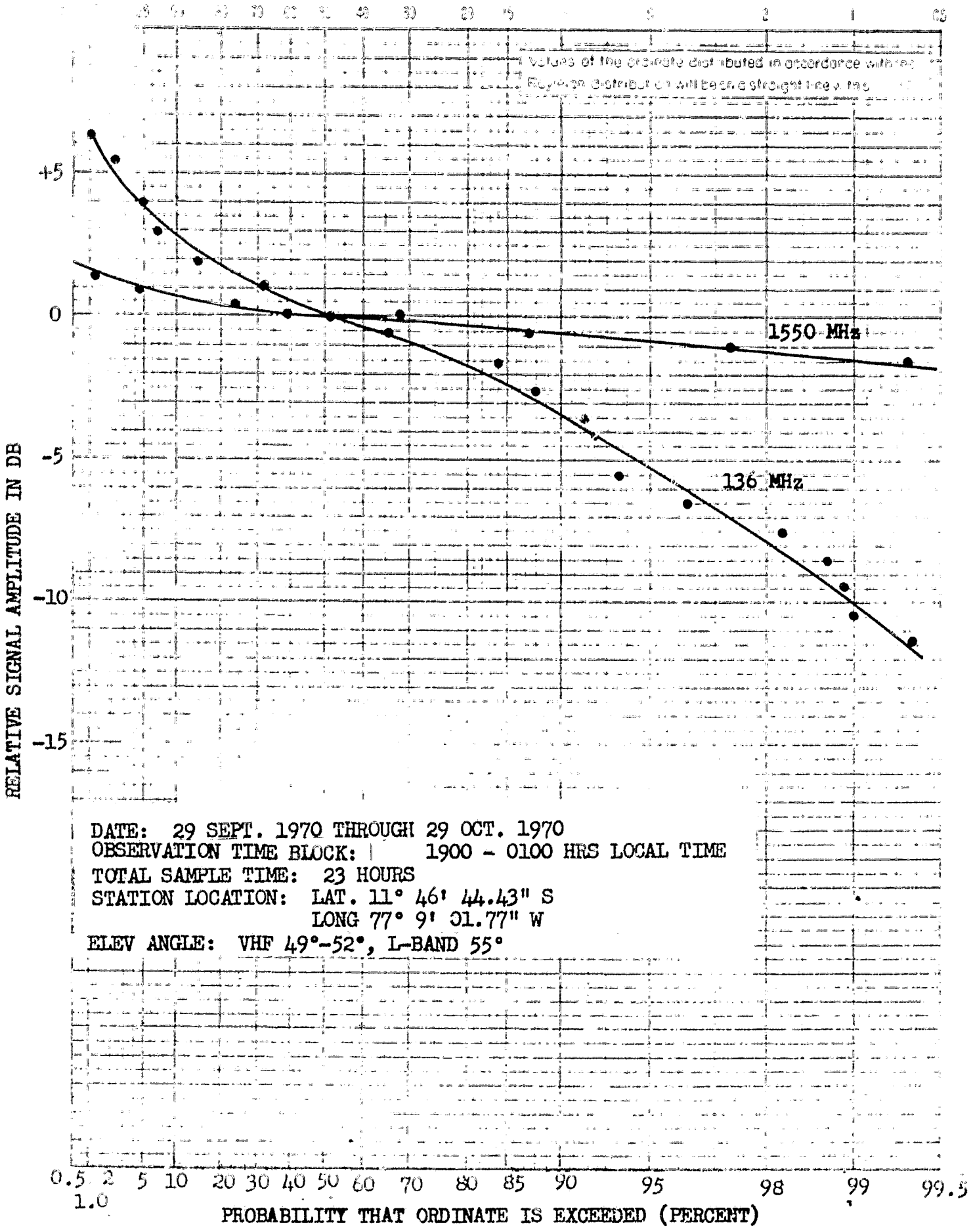

Figure 3 Cumulative Amplitude Distribution of ATS-5 and Intelsat I Signals (All Runs)

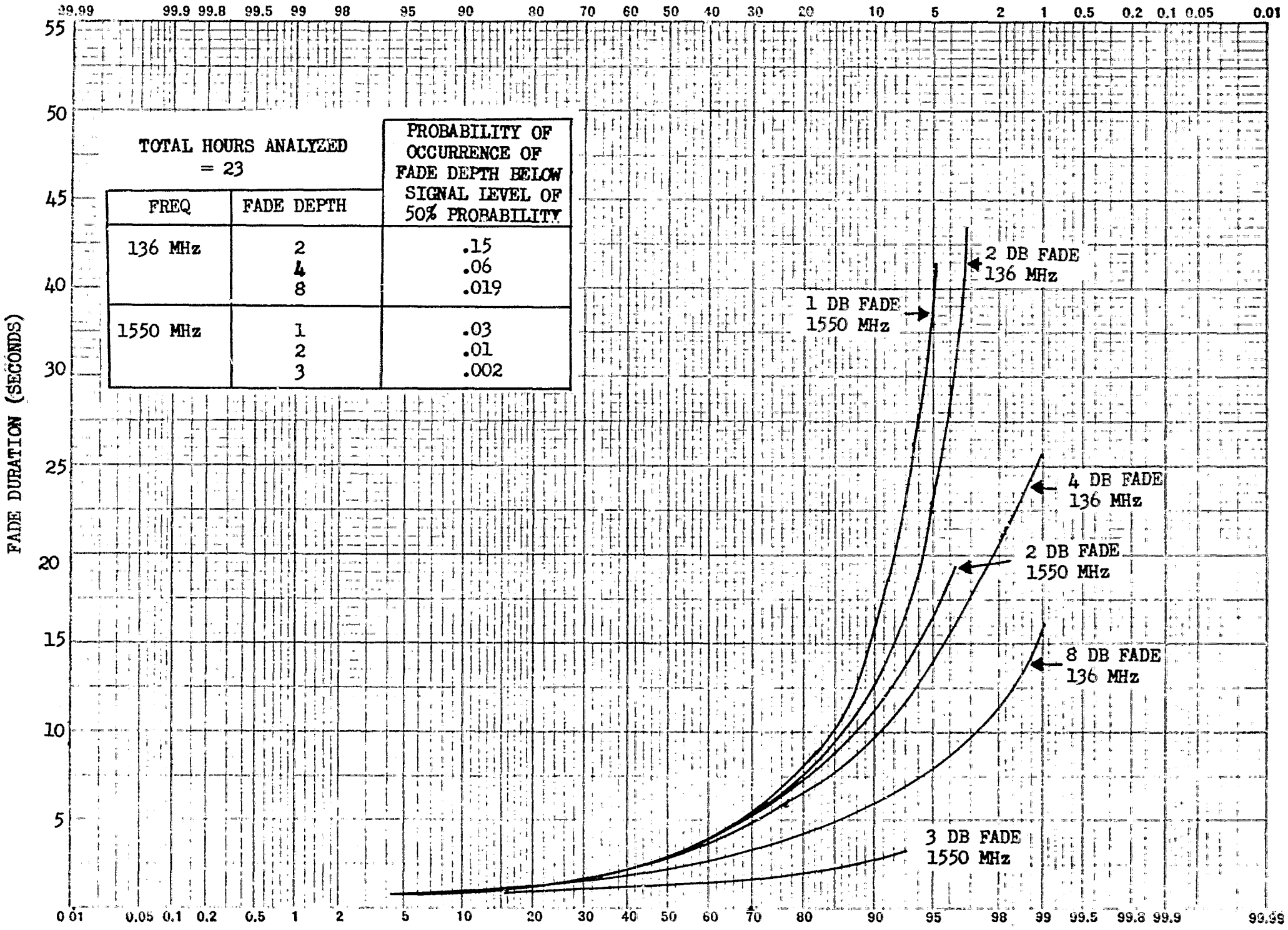

Figure 4 Probability That the Duration of a Given Fade Depth Will Not Exceed the Ordinate Value

RUN BY RUN
OBSERVED EXPONENT OF
FREQUENCY DEPENDENCE
BETWEEN 136 MHz AND
1550 MHz.

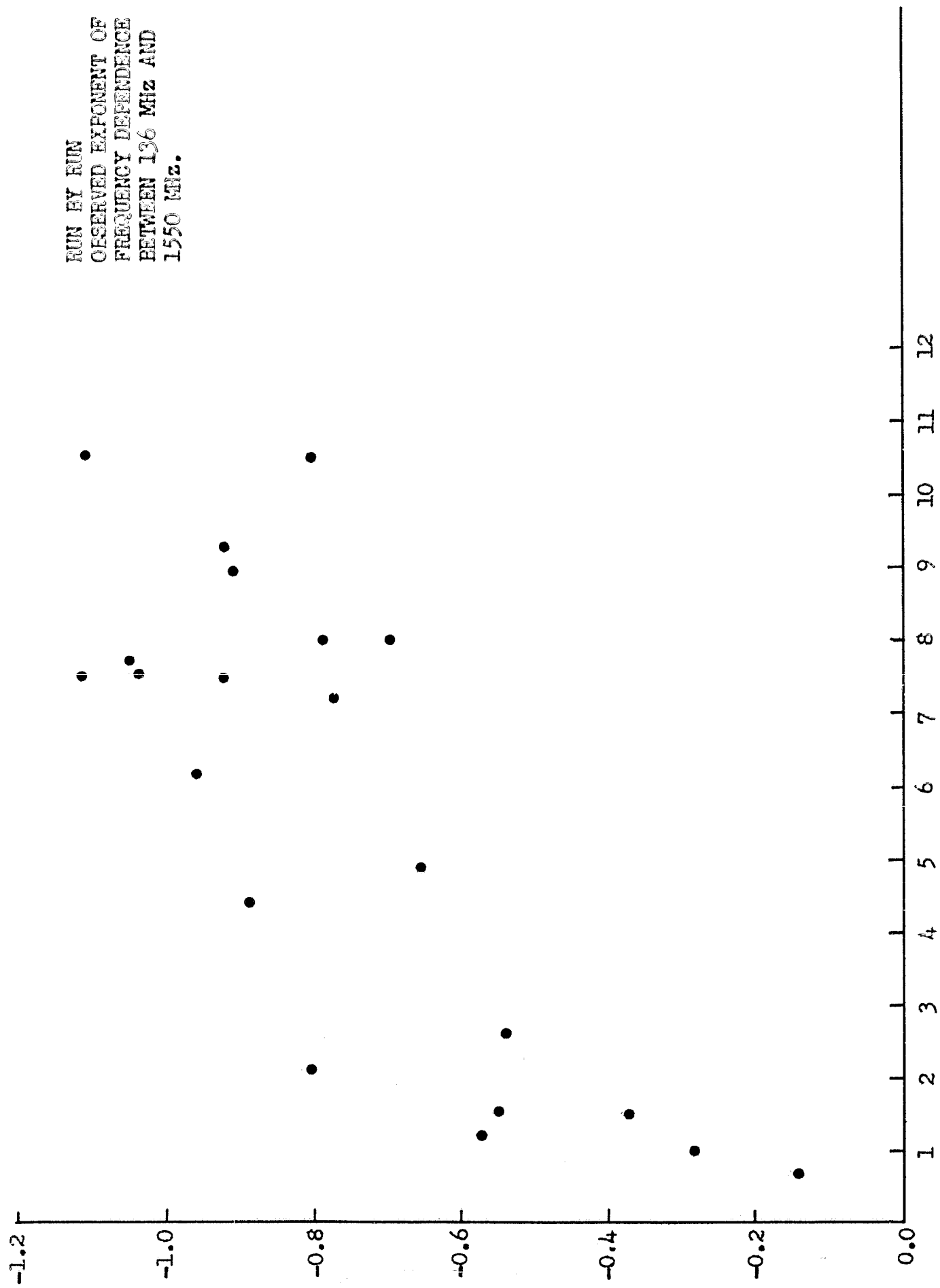

Figure 5 Scatter Diagram of Observed Exponent of Frequency Dependence

6.0 APPENDIX

Figure

A-1 Cumulative Amp. Dist. on 9-29-70

A-2 " " " on 10-2-70

A-3 " " " on 10-6-70

A-4 " " " on 10-8-70

A-5 " " " on 10-10-70

A-6 VHF Station Test Configuration

A-7 L-Band Station Test Configuration

A-8 Typical Strip Chart Summary

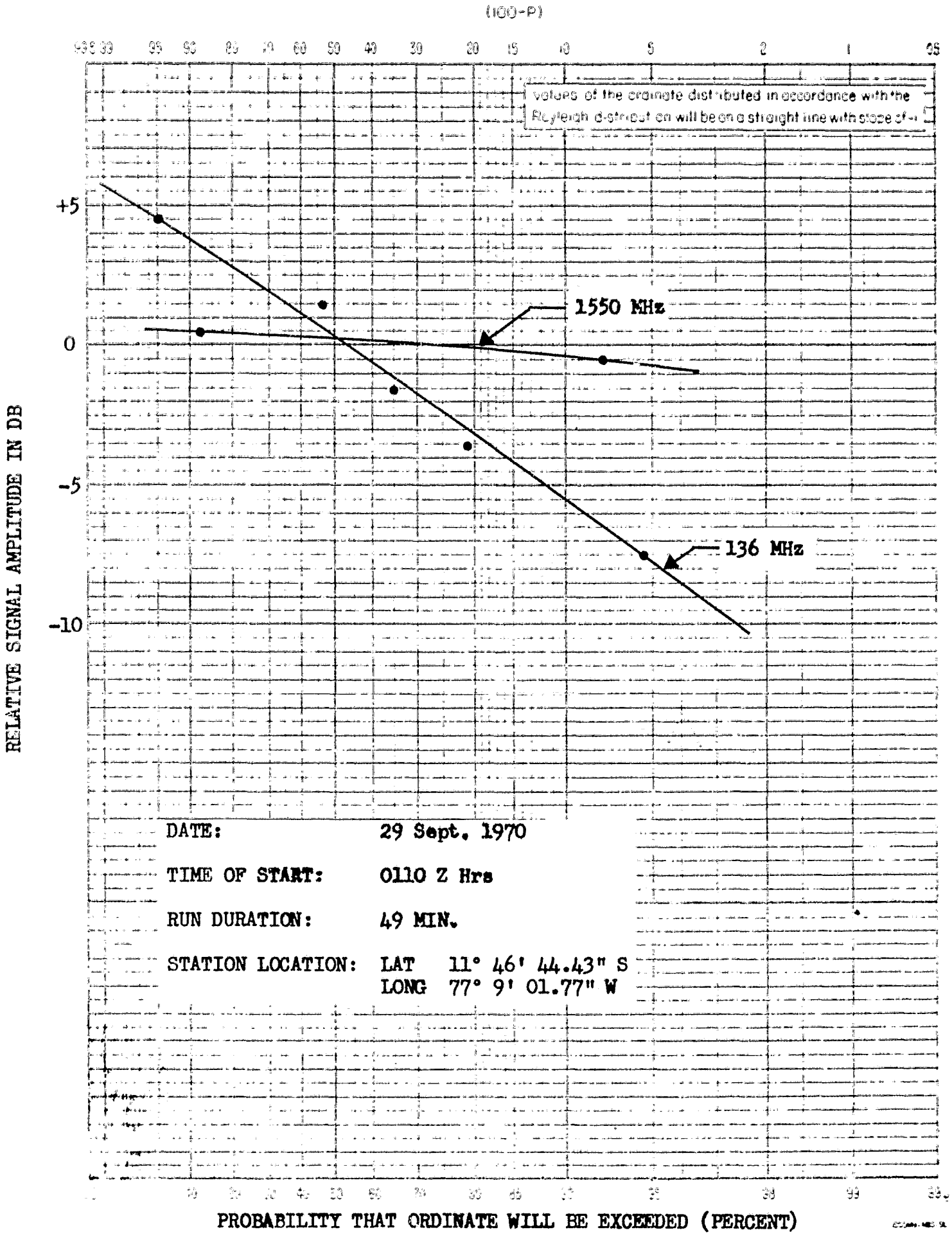

Figure A-1 Cumulative Amplitude Distribution of ATS-5 and Intelsat I Signals

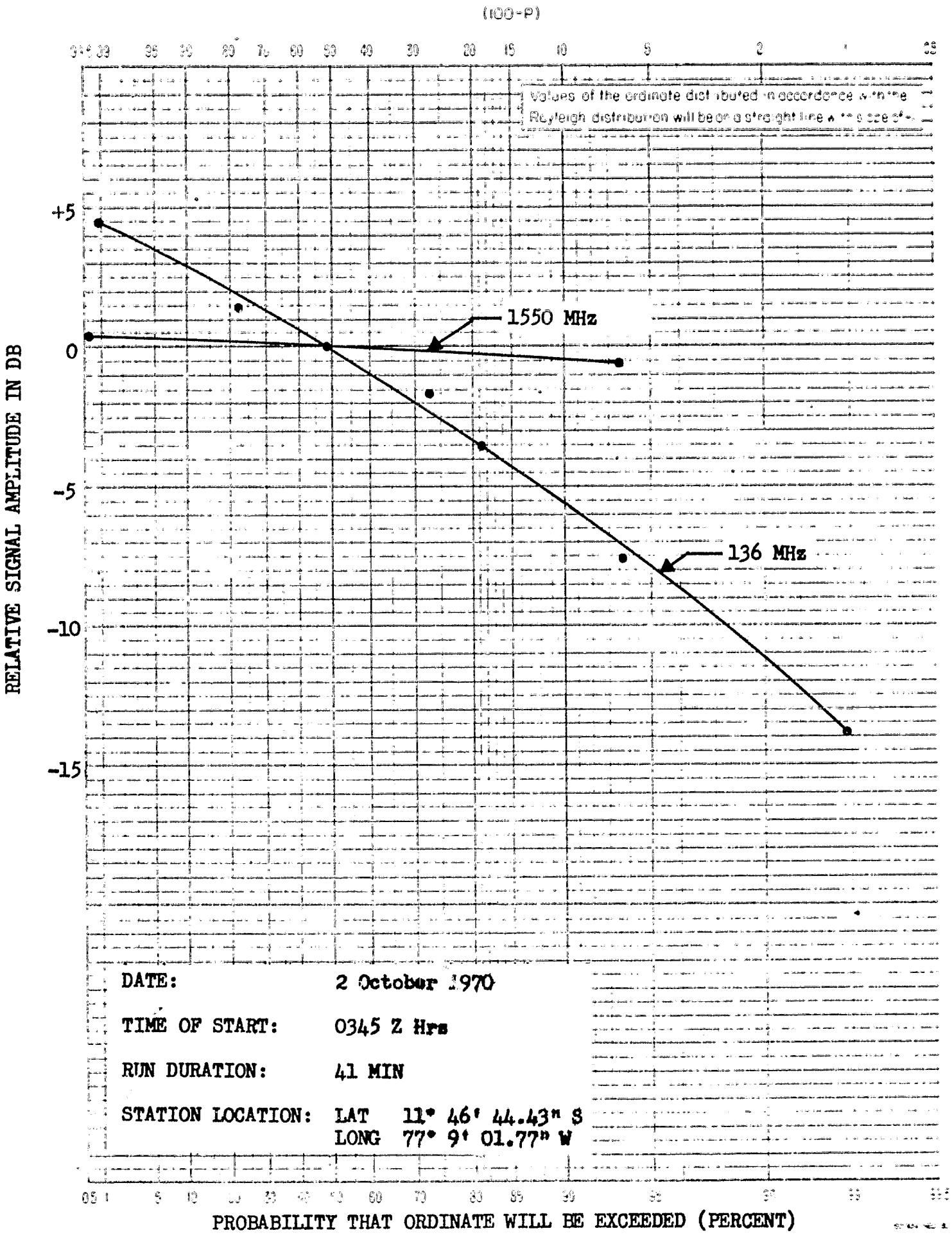

Figure A-2 Cumulative Amplitude Distribution of ATS-5 and Intelsat I Signals

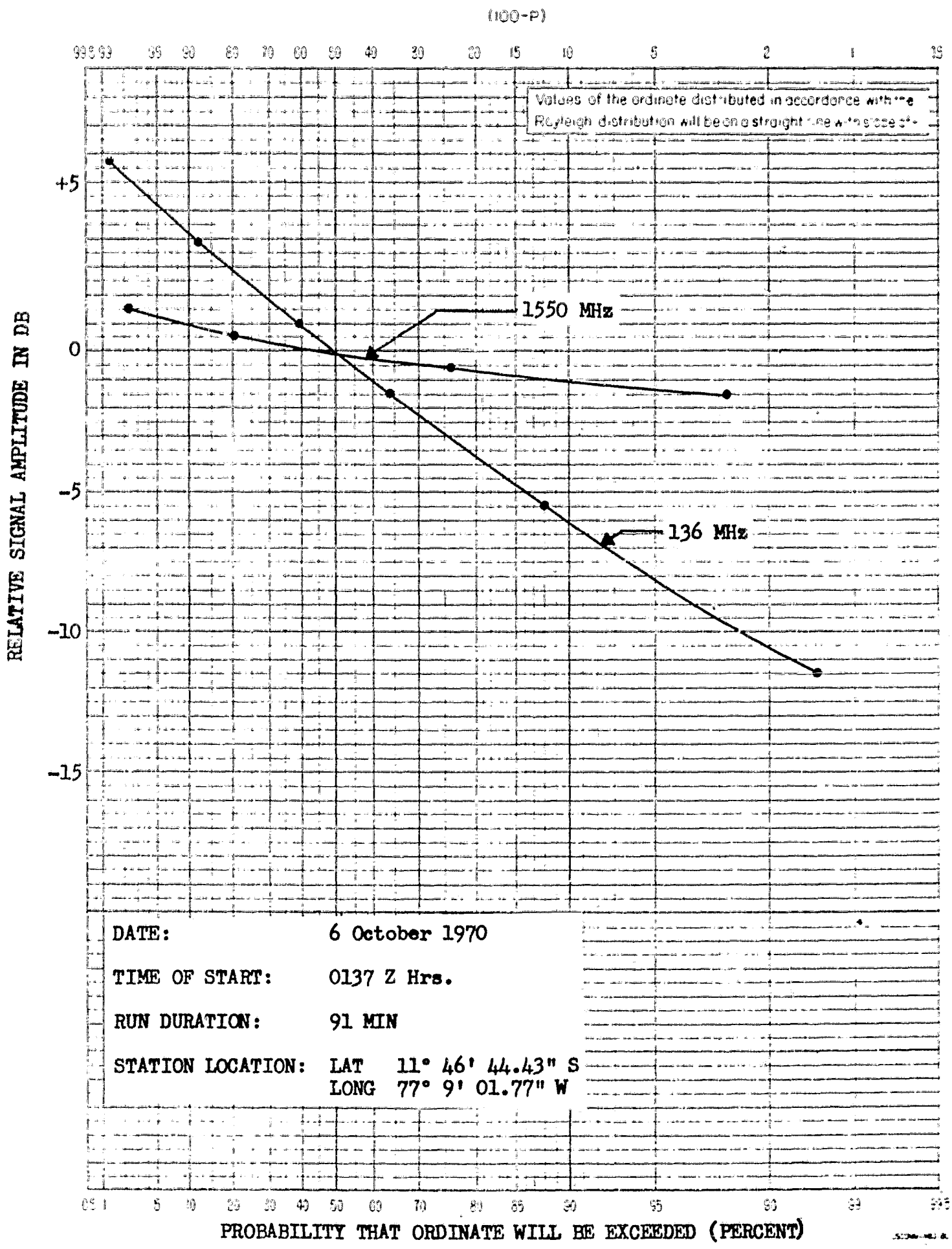

Figure A-3 Cumulative Amplitude Distribution of ATS-5 and Intelsat I Signals

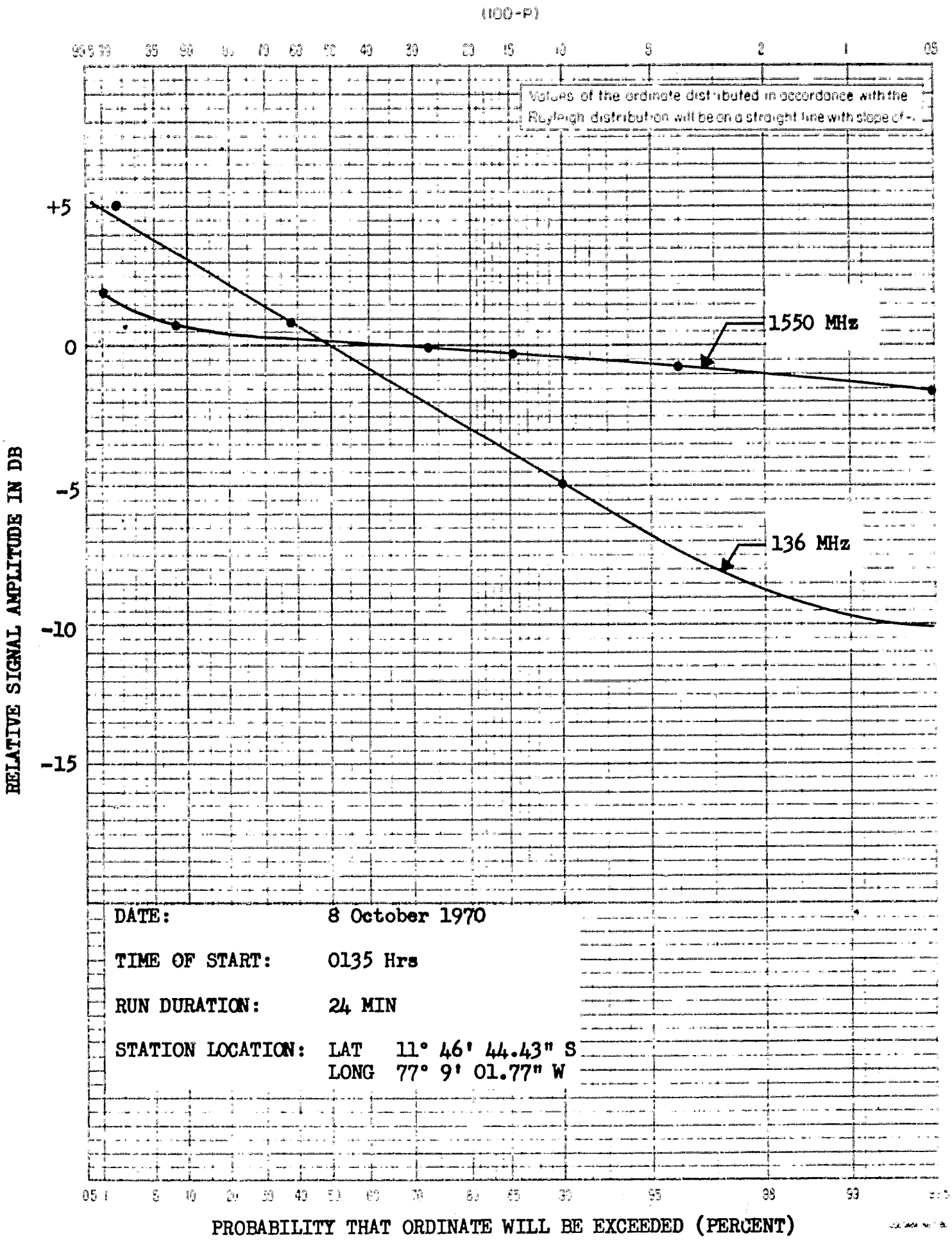

Figure A-4 Cumulative Amplitude Distribution of ATS-5 and Intelsat I Signals

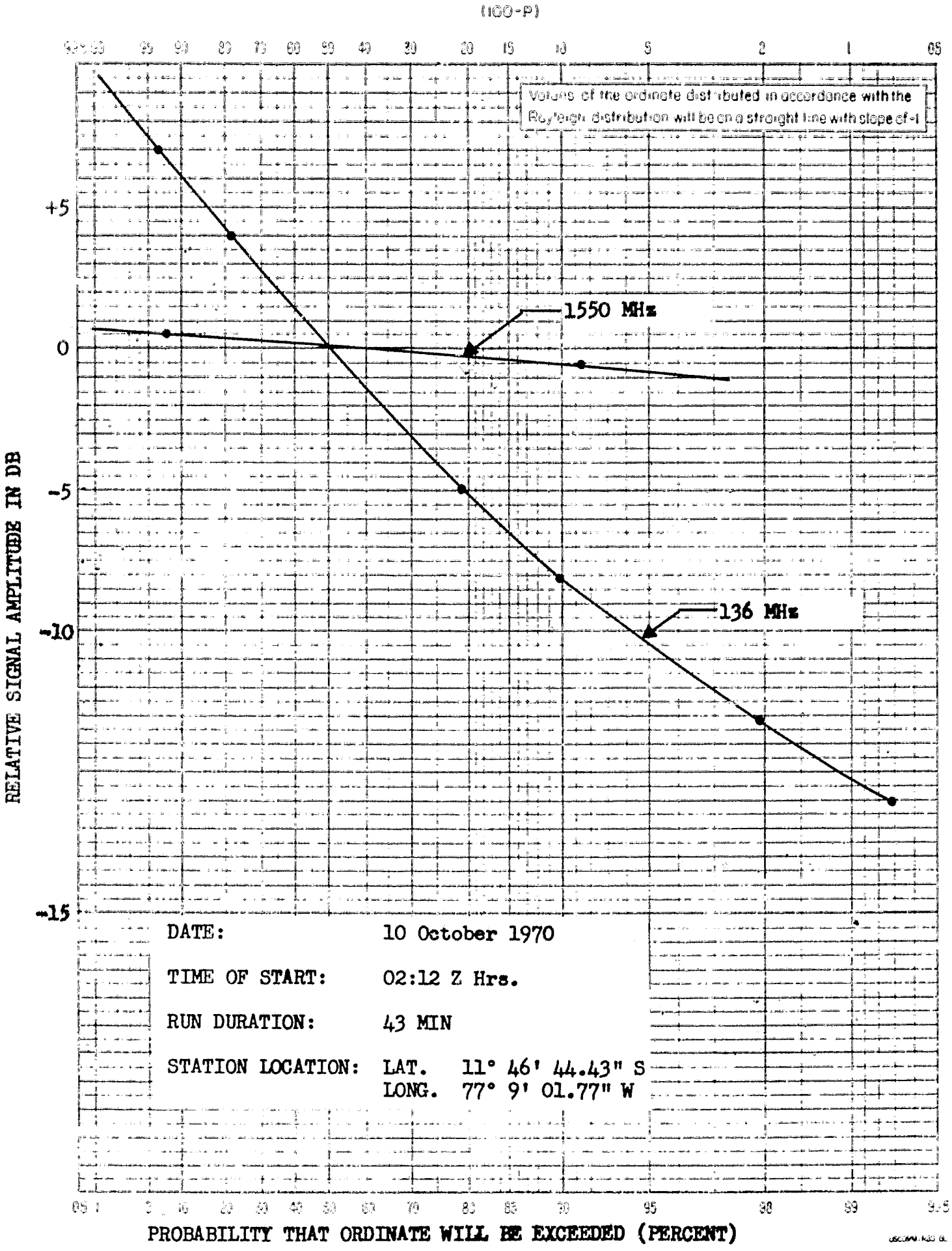

Figure A-5 Cumulative Amplitude Distribution of ATS-5 and Intelsat I Signals

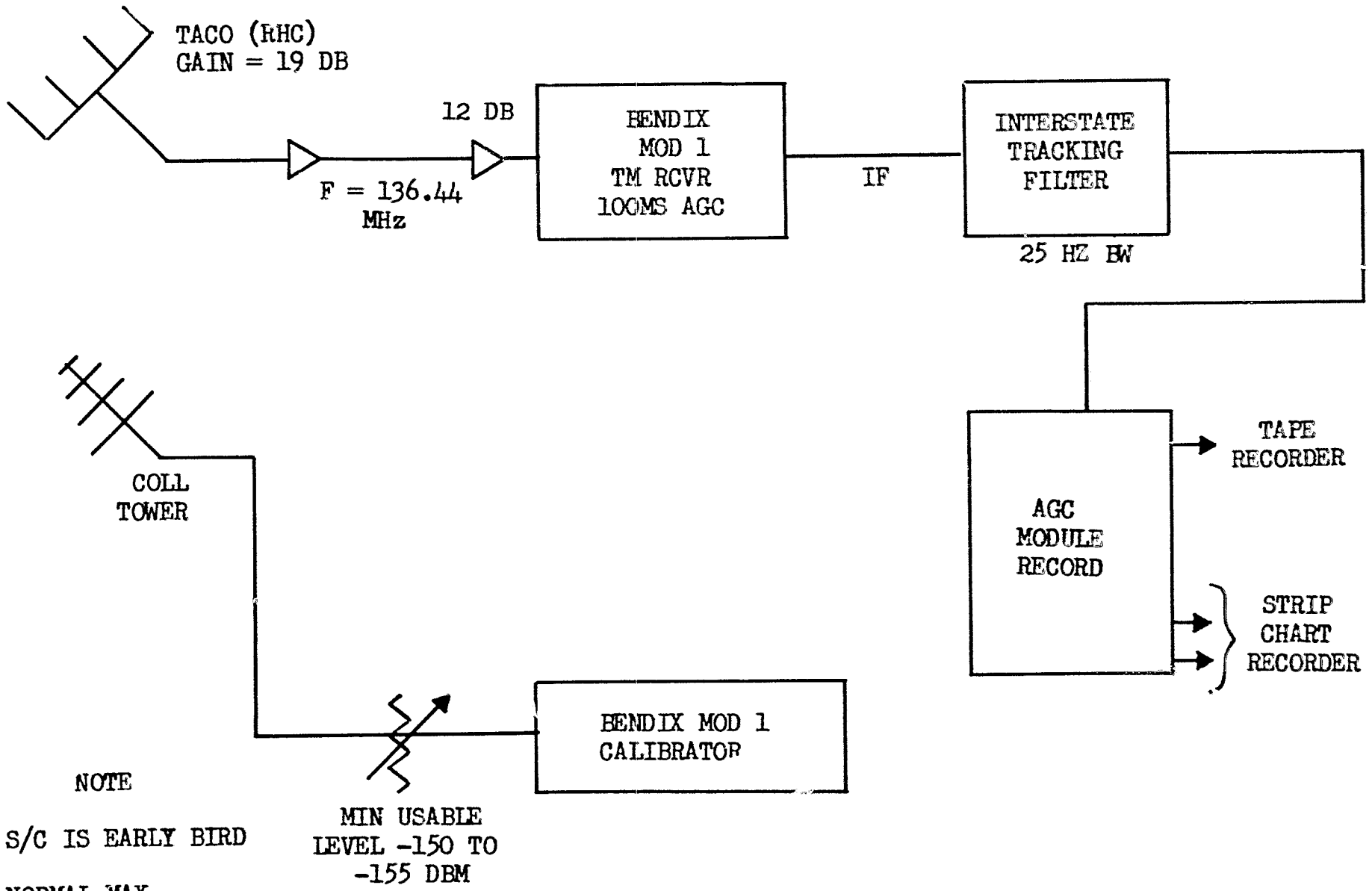

Figure A-6 VHF Station Test Configuration

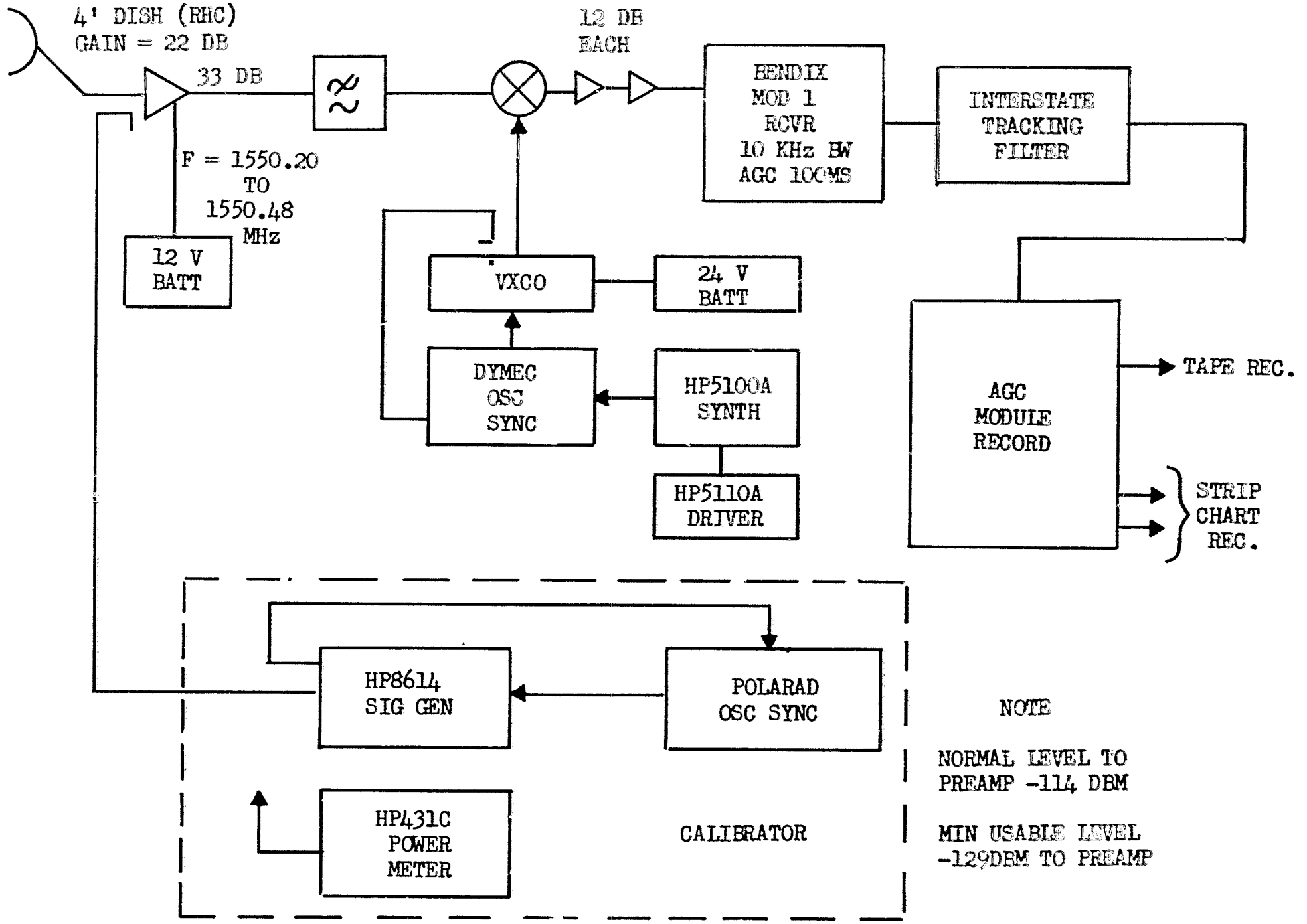

Figure A-7 L Band Station Test Configuration

Date: 29 Sept. 1970

Station: Lima

Time: 00052 - 0206Z

Tape No.: 001

Calibration	Pre	Post
L-Band	yes	agree within a 1 db
VHF	yes	within a 1 db

Commentary:

0022Z 29 Sept. '70	Both VHF and "L" band data VHF scin. less than 5 db "L" band scin. less than 2 db
0036Z	"L" band freq. drift drop data
0043Z	"L" band freq. retuned start data
0050Z	"L" band a drop of 2 db data spurious on one channel
0057Z	VHF begins 15-20 db fades and scin. "L" band less than 1 db-2 db
0059Z	VHF begins 20-25 db scin.
0102Z	VHF cal.
0104Z	"L" band cal.
0109Z	data begins VHF exp. 25 db fades or scin.
0118Z	"L" band less than 2 db VHF begin 20-30 db fades and scin. "L" band remains less than 2 db
0134	"L" band begins 2 db scin.
0141	"L" band scin less than 1 db
0202	VHF remains 20 db scin end of useful data

Figure A-8 Typical Strip Chart Summary